Available online at www.sciencedirect.com
ScienceDirect
Journal of Computational Physics 227 (2008) 5144–5159
JOURNAL OF COMPUTATIONAL PHYSICS
www.elsevier.com/locate/jcp

An All-Speed Roe-type scheme and its asymptotic analysis of low Mach number behaviour

Xue-song Li *, Chun-wei Gu

Key Laboratory for Thermal Science and Power Engineering of Ministry of Education, Department of Thermal Engineering, Tsinghua University, Beijing 100084, PR China

Received 8 June 2007; received in revised form 17 January 2008; accepted 23 January 2008
Available online 2 February 2008

Abstract

A new scheme, All-Speed-Roe scheme, was proposed for all speed flows. Compared with traditional preconditioned Roe scheme, All-Speed-Roe scheme changes non-linear eigenvalues in the numerical dissipation terms of Roe-type schemes. With an asymptotic analysis, the low Mach number behaviour of the scheme is studied theoretically in two ways. In one way, All-Speed-Roe scheme is regarded as finite magnification of Low-Speed-Roe scheme in the low Mach number limit. In the other way, a general form of All-Speed-Roe scheme is analyzed. Both ways demonstrate that All-Speed-Roe scheme has the same low Mach number behaviour as the original governing equation in the continuous case, which includes three important features: pressure variation scales with the square of the Mach number, the zero order velocity field is subject to a divergence constraint, and the second order pressure satisfies a Poisson-type equation in the case of constant-entropy. The analysis also leads to an unexpected conclusion that the velocity filed computed by traditional preconditioned Roe scheme does not satisfy the divergence constraint as the Mach number vanishes. Moreover, the analysis explains the reason of checkerboard decoupling and shows that momentum interpolation method provides a similar mechanism as traditional preconditioned Roe scheme inherently possesses to suppress checkerboard decoupling. In the end, general rulers for modifying non-linear eigenvalues are obtained. Finally, several numerical experiments are provided to support the theoretical analysis. All-Speed-Roe scheme has a sound foundation and is expected to be widely studied and applied to all speed flow calculations.

Keywords: All-Speed-Roe scheme; Asymptotic analysis; Shock-capturing scheme; Low Mach number; Checkerboard decoupling

1. Introduction

Shock-capturing schemes and time-marching algorithms are widely used in computation of compressible flows. For nearly incompressible flows, however, these technologies meet the problem of the large disparity between the fluid speed u and the acoustic speed c, which leads to both difficult convergence and deteriorated accuracy. In fact, the mathematic natures of compressible and incompressible flows are different, with their

* Corresponding author. Tel.: +86 10 62781739; fax: +86 10 62795946.
E-mail address: xs-li@mail.tsinghua.edu.cn (X.-s. Li).

0021-9991/$ - see front matter © 2008 Elsevier Inc. All rights reserved.
doi:10.1016/j.jcp.2008.01.037

respective hyperbolic and elliptic systems of governing partial differential equations. This is why flow fields are usually subdivided into compressible and incompressible ones in fluid mechanics, and corresponding computational methods are developed with relative independence. As a result, current flow solvers based on compressible flow methods are not suitable for incompressible flows, and vice versa. However, engineers prefer to use a unique code for varying flow conditions. Moreover, many problems contain both nearly incompressible flow regions with very low Mach numbers and decidedly compressible flow regions even with shocks, such as flows around turbomachinery blades at high angle of attack or in strongly convergent nozzles. For such problems, the compressible flow equations must be used throughout all the flow regions. Therefore, a general method for all flow speeds is of great practical and theoretical interest.

As an important algorithm to make shock-capturing and time-marching schemes effective for nearly incompressible flows, preconditioning methods [1–6] have been developed over the past decade, which provide a powerful remedy for the accuracy and convergence problems of schemes designed for compressible flows. Preconditioning methods provide that time derivatives are pre-multiplied by a matrix. Therefore, the effect of acoustic speed is slowed down towards the fluid speed.

However, in practice, most of previous preconditioned schemes [2–6] adopted the cut-off strategy as mentioned in Eq. (14) below that limits the capability of accurate simulating mixed low-speed/high-speed flows [3], or else preconditioned schemes are unstable unless the time step is extremely small, especially for viscous flows. This numerical phenomenon has been shown by numerical experiments [15,16], and some stability analyses are presented [7,15–17]. As an attempt to remedy this deficiency, a new scheme, All-Speed-Roe scheme, is developed based on preconditioning technique [8]. This scheme can use reasonable time steps without adopting the cut-off strategy to numerical dissipation. Compared with preconditioned schemes, the new scheme is easier for programming, more robust in computation of viscous flows and more accurate spatially. All-Speed-Roe scheme contains such an idea: numerical dissipations of Roe-type shock-capturing schemes can be modified for all flow speeds through changing the non-linear eigenvalues only. This partly empirical assumption may cause suspicion about the rationality of All-Speed-Roe scheme. For high-Mach-number flows, its rationality is easily convinced because All-Speed-Roe scheme becomes Roe scheme almost. The doubt mainly focuses on the behaviour of All-Speed-Roe scheme in the low Mach number limit. Therefore, besides the numerical examples provided in Ref. [8], a mathematic proof is still needed urgently to strengthen its theoretical foundation for this scheme to be widely accepted.

In this work, asymptotic analysis is adopted to research the behaviour of All-Speed-Roe scheme in the low Mach number limit. Asymptotic analysis is an important method to study the flow behaviour at low Mach numbers. A single scale asymptotic analysis was employed by Klainerman and Majda [9] to investigate the transition from the continuous compressible to the continuous incompressible regime. Later on, Klein [10] proposed a multiple length scale analysis to study the numerical behaviour of low Mach number flows. Recently, asymptotic analysis is used to demonstrate that shock-capturing schemes, such as Roe scheme [5], Godunov-type schemes [6], and AUSMDV scheme [11], produce unphysical discrete results but their corresponding preconditioned schemes have the correct scaling of pressure fluctuations when $M \to 0$.

The outline of this paper is as follows. Section 2 gives the governing equations with their non-dimensionalization and asymptotic expansion and the results for continuous case under the constant-entropy condition. Section 3 briefly reviews Roe scheme, the preconditioned Roe scheme, the Low-Speed-Roe scheme that is the basic of All-Speed-Roe scheme, and All-Speed-Roe scheme. Section 4 provides two ways to demonstrate the behaviour of All-Speed-Roe scheme in the low Mach number and constant entropy limit. In this chapter, an asymptotic analysis leads to the general formation of All-Speed-Roe scheme and the problem of checkerboard decoupling is also analyzed in detail. Section 5 gives some numerical experiments to support theoretical analysis. Finally, Section 6 closes the paper with some concluding remarks.

2. Governing equations and asymptotic expansion

2.1. Euler compressible equations

For simplicity, the two-dimensional Euler compressible equations are written as

$$\frac{\partial \boldsymbol{Q}}{\partial t}+\frac{\partial \boldsymbol{F}}{\partial x}+\frac{\partial \boldsymbol{G}}{\partial y}=0 \tag{1}$$

where: $\boldsymbol{Q}=[\rho \quad \rho u \quad \rho v \quad \rho E]^{\mathrm{T}}$, $\boldsymbol{F}=[\rho u \quad \rho u^2+p \quad \rho uv \quad u(\rho E+p)]^{\mathrm{T}}$, $\boldsymbol{G}=[\rho v \quad \rho uv \quad \rho v^2+p \quad v(\rho E+p)]^{\mathrm{T}}$, ρ is the fluid density, u, v are the velocity components in Cartesian coordinates (x,y), respectively, p is the pressure and E is the total energy.

2.2. Asymptotic expansion

As the first step in asymptotic expansion, the governing equations are non-dimensionalized respect to parameters $\rho^*=\max(\rho)$, $\boldsymbol{u}^*=\max(|\vec{\boldsymbol{u}}|)$, and the sound speed scale $c^*=\sqrt{\gamma \max(p)/\rho^*}$, with the non-dimensional flow variables defined as follows:

$$\tilde{\rho}=\frac{\rho}{\rho^*},\quad \tilde{p}=\frac{p}{\rho^*(c^*)^2},\quad \tilde{u}=\frac{u}{u^*},\quad \tilde{v}=\frac{v}{u^*},\quad \widetilde{E}=\frac{E}{(c^*)^2},\quad \tilde{x}=\frac{x}{x^*},\quad \tilde{t}=\frac{tu^*}{x^*} \tag{2}$$

where x^* is an arbitrary length scale.

Then the variables are asymptotically expanded into powers of the reference Mach number $M^*=u^*/c^*$:

$$\tilde{\phi}=\tilde{\phi}_0+M_*\tilde{\phi}_1+M_*^2\tilde{\phi}_2+M_*^3\tilde{\phi}_3+\cdots \tag{3}$$

where ϕ represents one of the fluid variables, i.e. ρ, u, v, E, or p and the superscript $\sim$ will be dropped in the following text for convenience.

By substituting expressions (2) and (3) into the continuous Eq. (1), Ref. [5] proves that the behaviour of the flow variables in the continuous case includes at least three important features as follows:

(1) The pressure varies in space asymptotically with the square of the reference Mach number:

$$p(x,t)=P_0(t)+M_*^2p_2(x,t) \tag{4}$$

This means that both p_0 and p_1 in the expansion of p are constant in space for the continuous cases.

(2) The velocity field is subject to a divergence constraint as the Mach number vanishes:

$$\mathrm{div}(\vec{\boldsymbol{u}}_0)=0 \tag{5}$$

(3) The second order pressure satisfies a Poisson-type equation that is closely related to the divergence constraint for velocity and the constant constraint for density:

$$\nabla^2 p_2=f(\vec{\boldsymbol{x}},\vec{\boldsymbol{u}}_0,\rho^0) \tag{6}$$

It should be noticed that Eq. (6) holds only if $\rho^0=Cte$. However, Ref. [10] points out that any low- or zero-Mach number flow that has non-constant entropy also has non-constant density. Therefore, the discussion about Eq. (6) in this paper is restricted to cases with constant-entropy.

Eq. (4) is the most important flow behaviour in discrete cases, and is researched in all related papers about preconditioned schemes such as Refs. [5,6,11]. However, those papers suffer from lack of depth in analyzing Eqs. (5) and (6), which will also be researched in this paper.

3. Numerical schemes

3.1. The general form of schemes and discussion of the central term

Many schemes including Roe scheme can be expressed as the sum of a central term and a numerical dissipation term:

$$\widetilde{\boldsymbol{F}}=\widetilde{\boldsymbol{F}}_{\mathrm{c}}+\widetilde{\boldsymbol{F}}_{\mathrm{d}} \tag{7}$$

Eq. (7) is the general form of schemes, in which $\widetilde{\boldsymbol{F}}_{\mathrm{c}}$ is the central term and $\widetilde{\boldsymbol{F}}_{\mathrm{d}}$ the numerical dissipation term.

For simplicity, in what follows equations of scheme are given for the i-direction with the index j omitted. In general, the central term $\widetilde{\boldsymbol{F}}_{\mathrm{c}}$ is expressed as

$$\widetilde{\boldsymbol{F}}_{\mathrm{c},i+\frac{1}{2}} = \frac{1}{2}(F_i + F_{i+1}) \tag{8}$$

$\widetilde{\boldsymbol{F}}_{\mathrm{c}}$ can also be expressed as other forms for different considerations. For example, in order to avoid velocity-pressure checkerboard decoupling, Ref. [13] proposes a form of momentum interpolation by adding a pressure stabilization term to the interface fluid velocity as done in Ref. [12]. The form is

$$\widetilde{\boldsymbol{F}}^{\mathrm{press}}_{\mathrm{c},i+\frac{1}{2}} = U_{\mathrm{c}}\widehat{\boldsymbol{Q}}_{i+\frac{1}{2}} + \boldsymbol{P}_{i+\frac{1}{2}} \tag{9}$$

where $U_{\mathrm{c}} = \left(\boldsymbol{u}_{i+\frac{1}{2},L} + u_{i+\frac{1}{2},R}\right)/2 - c_2/(\rho^* u^*)\left(p_{i+\frac{1}{2},R} - p_{i+\frac{1}{2},L}\right)$, $\widehat{\boldsymbol{Q}} = [\rho \quad \rho u \quad \rho v \quad \rho E + p]^{\mathrm{T}}, \boldsymbol{P} = [0 \quad p \quad 0 \quad 0]^{\mathrm{T}}$, and c_2 is a constant that should be chosen as small as possible for the accuracy reason. For the stability reason, however, Ref. [13] recommends that c_2 should be larger than a threshold value 0.04.

For simplicity, it is default to use Eq. (8) as the central term in the next unless otherwise specified, because the main difference between schemes lies in the numerical dissipation term, which will be discussed below.

3.2. Roe scheme and preconditioned Roe scheme

For "classical" Roe scheme, the numerical dissipation term can be expressed as

$$\widetilde{\boldsymbol{F}}^{\mathrm{Roe}}_{\mathrm{d},i+\frac{1}{2}} = -\frac{1}{2}\boldsymbol{R}_{i+\frac{1}{2}}\left|\boldsymbol{\Lambda}_{i+\frac{1}{2}}\right|\boldsymbol{R}^{-1}_{i+\frac{1}{2}}(\boldsymbol{Q}_{i+1} - \boldsymbol{Q}_i) \tag{10}$$

where $\boldsymbol{R}$ is the right eigenvector matrix of $\frac{\partial \boldsymbol{F}}{\partial \boldsymbol{Q}}$ and $\boldsymbol{\Lambda}$ the diagonal matrix formed with relevant eigenvalues:

$$\lambda_{1,2} = u \quad \text{and} \quad \lambda_{3,4} = u \pm c \tag{11}$$

For preconditioned Roe scheme (denoted by Pre-Roe scheme):

$$\widetilde{\boldsymbol{F}}^{\mathrm{P\text{-}Roe}}_{\mathrm{d},i+\frac{1}{2}} = -\frac{1}{2}\Gamma^{-1}_{i+\frac{1}{2}}\widehat{\boldsymbol{R}}_{i+\frac{1}{2}}\left|\widehat{\boldsymbol{\Lambda}}_{i+\frac{1}{2}}\right|\widehat{\boldsymbol{R}}^{-1}_{i+\frac{1}{2}}(\boldsymbol{Q}_{i+1} - \boldsymbol{Q}_i) \tag{12}$$

where $\boldsymbol{\Gamma} = \frac{\partial \boldsymbol{Q}}{\partial \boldsymbol{W}}\boldsymbol{\Gamma}_0\frac{\partial \boldsymbol{W}}{\partial \boldsymbol{Q}}$ is the preconditioner based on conservation variables with $\boldsymbol{\Gamma}_0 = \mathrm{diag}(\,\theta \quad 1 \quad 1 \quad 1\,)$ when $\boldsymbol{W}$ is a vector of primitive variables $[p \quad u \quad v \quad S]^{\mathrm{T}}$. When $\theta = 1$, Pre-Roe becomes "classical" Roe scheme. $\widehat{\boldsymbol{R}}$ is the right eigenvector matrix of $\boldsymbol{\Gamma}\frac{\partial \boldsymbol{F}}{\partial \boldsymbol{Q}}$ and $\widehat{\boldsymbol{\Lambda}}$ is the diagonal matrix formed with relevant eigenvalues:

$$\hat{\lambda}_{1,2} = u \quad \text{and} \quad \hat{\lambda}_{3,4} = u' \pm c' = \frac{1}{2}\left[(1+\theta)u \pm \sqrt{4c^2\theta + (1-\theta)^2u^2}\right] \tag{13}$$

In theory, the key factor θ should relate to the local Mach number. However, in order to avoid computational instability, θ is cut-off by the global Mach number:

$$\theta = \min[\max(KM^2_{\mathrm{ref}}, M^2), 1] \tag{14}$$

where the constant K is typically equal to 1, and the reference Mach number M_{ref} is the global Mach number, which may be the inlet Mach number, the average Mach number, or the maximum Mach number over the flow. This means that the accuracy can be high enough in high-speed flow regions, such as the main flow, but will be deteriorated in low-speed flow regions, such as the boundary layers.

3.3. Low-Speed-Roe scheme

The computational instability of preconditioning technique is due to the eigenvector matrix [14] and the structure of $\frac{1}{\theta}$ in the eigenvector matrix [15,16]. Therefore, Low-Speed-Roe scheme is derived from Roe scheme based on preconditioning technology for low speed flow condition as [8,15,16]:

$$\widetilde{\boldsymbol{F}}^{\text{L-Roe}}_{\text{d},i+\frac{1}{2}} = -\frac{1}{2}\left|u_{i+\frac{1}{2}}\right|[\rho_{i+1}-\rho_i, \rho_{i+1}u_{i+1}-\rho_i u_i, \rho_{i+1}v_{i+1}-\rho_i v_i, \gamma(\rho_{i+1}E_{i+1}-\rho_i E_i)]^{\mathrm{T}}$$
$$\approx -\frac{1}{2}\left|u_{i+\frac{1}{2}}\right|(\boldsymbol{Q}_{i+1}-\boldsymbol{Q}_i) \tag{15}$$

This scheme is similar to the simplified AUSM+ scheme [13] for large eddy simulation (LES), in that their numerical dissipations are both proportional to the local fluid speed. Namely, Low-Speed-Roe scheme has good uniform accuracy both in the boundary layers and in the main flow.

However, Low-Speed-Roe scheme is only tailored for globally low speed flows without the effect of acoustic speed on the numerical dissipation term. All-Speed-Roe scheme is, therefore, proposed in next section to overcome this limitation while holding the advantage of uniform accuracy.

3.4. All-Speed-Roe Scheme

Now that "classical" Roe scheme is suitable for high-Mach-number flows as well known while Low-Speed-Roe scheme is effective for low Mach number flows as shown above, All-Speed-Roe scheme is proposed, which combines the advantages of the two schemes by introducing a function of the local Mach number [8] as

$$\widetilde{\boldsymbol{F}}^{\text{A-Roe}}_{\text{d},i+\frac{1}{2}} = -\frac{1}{2}\boldsymbol{R}_{i+\frac{1}{2}}\left|\boldsymbol{\Lambda}^{\text{A-Roe}}_{i+\frac{1}{2}}\right|\boldsymbol{R}^{-1}_{i+\frac{1}{2}}(\boldsymbol{Q}_{i+1}-\boldsymbol{Q}_i) \tag{16}$$

where $\boldsymbol{R}$ is the right eigenvector matrix of $\frac{\partial \boldsymbol{F}}{\partial \boldsymbol{Q}}$ consistent to that of "classical" Roe scheme (10), but the elements of the diagonal matrix $\boldsymbol{\Lambda}^{\text{A-Roe}}$ different from those in Eq. (11) are

$$\lambda^{\text{A-Roe}}_{1,2} = u \quad \text{and} \quad \lambda^{\text{A-Roe}}_{3,4} = u \pm f(M)c \tag{17}$$

The central term can otherwise be obtained by combining Eqs. (8) and (9) with the function $f(M)$ as shown in Ref. [8]:

$$\widetilde{\boldsymbol{F}}^{\text{A-Roe}}_{\text{c},i+\frac{1}{2}} = f(M)\widetilde{\boldsymbol{F}}_{\text{c},i+\frac{1}{2}} + [1-f(M)]\widetilde{\boldsymbol{F}}^{\text{press}}_{\text{c},i+\frac{1}{2}}$$

The factor $f(M)$ should be related to the local Mach number, because the numerical dissipation should change with the local Mach number based on the viewpoint of preconditioning methods. Three rules should be observed in choosing function $f(M)$:

1. $0 < f(M) < 1$ when $0 < M < 1$
2. $f(M) \to 0$ when $M \to 0$
3. $f(M) = 1$ when $M \geqslant 1$

A expression of $f(M)$ is recommended and shown in Eq. (18) and Fig. 1, which takes account of the relation of the fluid speed and acoustic speed in preconditioned eigenvalues in Eq. (13) and has been calibrated.

$$f(M) = \frac{c'}{u'}\frac{u}{c} = \min\left(M\frac{\sqrt{4+(1-M^2)^2}}{1+M^2}, 1\right) \tag{18}$$

Fig. 1 shows the effect of Mach number on the function $f(M)$ calculated from Eq. (18). Near shocks All-Speed-Roe scheme becomes "classical" Roe scheme because the value of $f(M)$ tends to 1 smoothly when $M \to 1$. This means that All-Speed-Roe scheme is valid for a compressible flow. For very low Mach number flows, $f(M)$ is adjusted almost proportionally to the local Mach number.

For All-Speed-Roe scheme, the cut-off strategy is no longer needed. It means that θ can be defined as $\theta = \min[M^2, 1]$ [8].

As to the behaviour in time of the scheme, we give a modified method to accelerate convergence for low Mach number steady flows [8]. Ref. [5] points out for unsteady flows that the temporal accuracy of the scheme is not affected when preconditioning is only used to modify the dissipation terms. It means that the variation of the spatial numerical dissipation has no effect on the temporal accuracy. Consequently, All-Speed-Roe

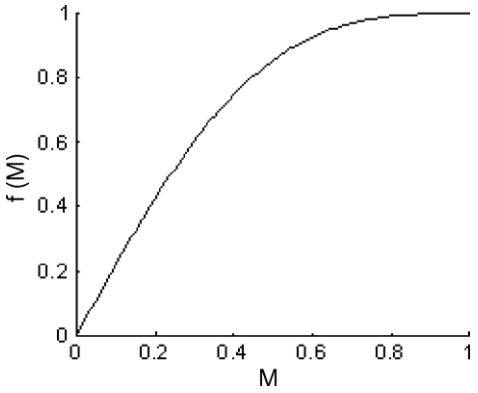

Fig. 1. Effect of Mach number on the function $f(M)$.

scheme can be directly applied to unsteady flows provided that the dissipation terms are modified with explicit multistage temporal discretization. However, explicit multistage method is subject to the stringent CFL time step constraints. Ref. [1] shows that the method of dual time stepping is a better choice for unsteady flows to obtain time-accurate solutions of the preconditioned equations. The method of dual time stepping is also good for All-Speed-Roe scheme for unsteady flows to obtain better convergence efficiency, because it can utilize accelerating convergence techniques developed for steady flows.

All-speed-Roe scheme is so simple and easy to use uniformly for all speed flows that we expect that it is potent to replace the traditional preconditioned schemes in all-speed flow calculations. Therefore, further research is desired to strengthen its theoretical foundation. The following mathematic proofs are given to address the doubt about the behaviour of All-Speed-Roe scheme in the low Mach number limit.

4. Asymptotic analysis of discretized cases

4.1. Low-Speed-Roe scheme

Firstly, we perform an asymptotic analysis, which is introduced by Ref. [5], on Low-Speed-Roe scheme used to approximate Euler Eq. (1). For simplicity, we consider a regular Cartesian mesh of uniform grid size δ, and we label neighbours of grid node $\boldsymbol{i}$ with sign $v(\boldsymbol{i}) = \{(i-1, j), (i+1, j), (i, j-1), (i, j+1)\}$. The cell associated with node $\boldsymbol{i}$ is $C_i = [i-1/2, i+1/2] \times [j-1/2, j+12]$, and $\vec{\boldsymbol{n}}_{il}$ is the unit normal vector on the interface between the cells associated with node $\boldsymbol{i}$ and node $\boldsymbol{l}$.

The following semi-discrete equations can be easily obtained by applying Low-Speed-Roe scheme Eq. (15) in a first-order finite volume context:

Continuity equation:

$$\delta\frac{\partial\rho_i}{\partial t}+\frac{1}{2}\sum_{l\in v(i)}\rho_l\vec{\boldsymbol{u}}_l\cdot\vec{\boldsymbol{n}}_{il}+\frac{1}{2}\sum_{l\in v(i)}|U_{il}|\Delta_{il}\rho=0 \tag{19}$$

Horizontal momentum equation:

$$\delta\frac{\partial\rho_i u_i}{\partial t}+\frac{1}{2}\sum_{l\in v(i)}\rho_l u_l\vec{\boldsymbol{u}}_l\cdot\vec{\boldsymbol{n}}_{il}+p_l(n_x)_{il}+\frac{1}{2}\sum_{l\in v(i)}|U_{il}|(u_{il}\Delta_{il}\rho+\rho_{il}\Delta_{il}u)=0 \tag{20}$$

Vertical momentum equation:

$$\delta\frac{\partial\rho_i v_i}{\partial t}+\frac{1}{2}\sum_{l\in v(i)}\rho_l v_l\vec{\boldsymbol{u}}_l\cdot\vec{\boldsymbol{n}}_{il}+p_l(n_y)_{il}+\frac{1}{2}\sum_{l\in v(i)}|U_{il}|(v_{il}\Delta_{il}\rho+\rho_{il}\Delta_{il}v)=0 \tag{21}$$

Energy equation:

$$\delta\frac{\partial\rho_i E_i}{\partial t}+\frac{1}{2}\sum_{l\in v(i)}(\rho_l E_l+p_l)\vec{\boldsymbol{u}}_l\cdot\vec{\boldsymbol{n}}_{il}+\frac{1}{2}\sum_{l\in v(i)}|U_{il}|(E_{il}\Delta_{il}\rho+\rho_{il}\Delta_{il}E)=0 \tag{22}$$

The state law of perfect gas is also needed:

$$p = RT\rho = (\gamma - 1)\left[\rho E - \frac{1}{2}\rho(u^2 + v^2 + w^2)\right] \tag{23}$$

In the above equations, $U = un_x + vn_y$, $\Delta_{il}\phi = \phi_i - \phi_l$, and ϕ_{il} denotes the Roe average of the states ϕ_i and ϕ_l.

On substituting the non-dimensional variables Eq. (2) into Eqs. (19)–(23), the dimensionless discrete equations are obtained:

$$\tilde{\delta}\frac{\partial \rho_i}{\partial t} + \frac{1}{2}\sum_{l\in v(i)} \rho_l \vec{\boldsymbol{u}}_l \cdot \vec{\boldsymbol{n}}_{il} + |U_{il}|\Delta_{il}\rho = 0 \tag{24}$$

$$\frac{1}{2M_*^2}\sum_{l\in v(i)} p_l (n_x)_{il} + \tilde{\delta}\frac{\partial \rho_i u_i}{\partial t} + \frac{1}{2}\sum_{l\in v(i)} \rho_l u_l \vec{\boldsymbol{u}}_l \cdot \vec{\boldsymbol{n}}_{il} + |U_{il}|(u_{il}\Delta_{il}\rho + \rho_{il}\Delta_{il}u) = 0 \tag{25}$$

$$\frac{1}{2M_*^2}\sum_{l\in v(i)} p_l (n_y)_{il} + \tilde{\delta}\frac{\partial \rho_i v_i}{\partial t} + \frac{1}{2}\sum_{l\in v(i)} \rho_l v_l \vec{\boldsymbol{u}}_l \cdot \vec{\boldsymbol{n}}_{il} + |U_{il}|(v_{il}\Delta_{il}\rho + \rho_{il}\Delta_{il}v) = 0 \tag{26}$$

$$\tilde{\delta}\frac{\partial \rho_i E_i}{\partial t} + \frac{1}{2}\sum_{l\in v(i)} (\rho_l E_l + p_l)\vec{\boldsymbol{u}}_l \cdot \vec{\boldsymbol{n}}_{il} + |U_{il}|(E_{il}\Delta_{il}\rho + \rho_{il}\Delta_{il}E) = 0 \tag{27}$$

$$p = (\gamma - 1)\left[\rho E - \frac{M_*^2}{2}\rho(u^2 + v^2 + w^2)\right] \tag{28}$$

Expansions of all the variables as powers of the reference Mach number M^* (Eq. (3)) are substituted into Eqs. (24)–(28), and the terms with equal powers of M^* are collected for research of the behaviour described in Eqs. (4)–(6):

(1) Order $1/M_*^2$

$$p^0_{i-1,j} - p^0_{i+1,j} = 0 \tag{29}$$

$$p^0_{i,j-1} - p^0_{i,j+1} = 0 \tag{30}$$

(2) Order $1/M^*$

$$p^1_{i-1,j} - p^1_{i+1,j} = 0 \tag{31}$$

$$p^1_{i,j-1} - p^1_{i,j+1} = 0 \tag{32}$$

(3) Order 1

$$\tilde{\delta}\frac{\partial \rho_i^0}{\partial t} + \frac{1}{2}\sum_{l\in v(i)} \rho_l^0 \vec{\boldsymbol{u}}_l^0 \cdot \vec{\boldsymbol{n}}_{il} + |U_{il}^0|\Delta_{il}\rho^0 = 0 \tag{33}$$

$$p^2_{i-1,j} - p^2_{i+1,j} = 2\tilde{\delta}\frac{\partial \rho_i^0 u_i^0}{\partial t} + \sum_{l\in v(i)} \rho_l^0 u_l^0 \vec{\boldsymbol{u}}_l^0 \cdot \vec{\boldsymbol{n}}_{il} + |U_{il}^0|(u_{il}^0\Delta_{il}\rho^0 + \rho_{il}^0\Delta_{il}u^0) \tag{34}$$

$$p^2_{i,j-1} - p^2_{i,j+1} = 2\tilde{\delta}\frac{\partial \rho_i^0 v_i^0}{\partial t} + \sum_{l\in v(i)} \rho_l^0 v_l^0 \vec{\boldsymbol{u}}_l^0 \cdot \vec{\boldsymbol{n}}_{il} + |U_{il}^0|(v_{il}^0\Delta_{il}\rho^0 + \rho_{il}^0\Delta_{il}v^0) \tag{35}$$

$$\tilde{\delta}\frac{\partial \rho_i^0 E_i^0}{\partial t} + \frac{1}{2}\sum_{l\in v(i)} (\rho_l^0 E_l^0 + p_l^0)\vec{\boldsymbol{u}}_l^0 \cdot \vec{\boldsymbol{n}}_{il} + |U_{il}^0|(E_{il}^0\Delta_{il}\rho^0 + \rho_{il}^0\Delta_{il}E^0) = 0 \tag{36}$$

The pressure behaviour (Eq. (4)) is studied at the first.

Eqs. (29) and (30) imply that p^0 has a chess-like four-field solution as shown in Fig. 2. In the viewpoint of physics, $A = B = C = D$. Therefore, $p_i^0 = cte\ \forall \boldsymbol{i}$.

However, in numerical simulation of low Mach number flows, it is not assured to avoid a four-field solution that leads to the classical problem of velocity-pressure checkerboard decoupling. This is why we need additional methods, such as staggered grids or momentum interpolation in collocated grids, to obtain the

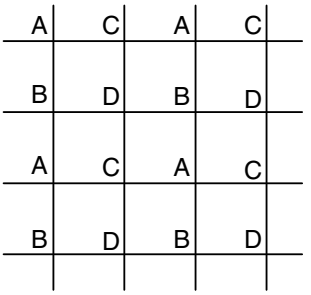

Fig. 2. Four-field solution.

physical solution. It is preferred to use momentum interpolation method as in Eq. (9) because it is easier to realize, although staggered grids method is more effective.

For the same reason, Eqs. (31) and (32) imply that $p_i^1 = cte\ \forall \boldsymbol{i}$ in physics.

Eqs. (34) and (35) indicate that the order M_*^2 pressure p^2 is not a constant. Therefore, the discrete solution by Low-Speed-Roe scheme supports pressure fluctuations of order M_*^2 (Eq. (4)):

$$p(x,t) = P_0(t) + M_*^2 p_2(x,t) \tag{37}$$

The velocity behaviour is then studied. The order 1 state law is

$$P_0 = (\gamma - 1)\rho^0 E^0 \tag{38}$$

According to Ref. [5], the pressure P_0 can be assumed as a constant in time as well as in space:

$$\frac{\mathrm{d}P_0}{\mathrm{d}t} = 0 \tag{39}$$

Consequently, $\rho^0 E^0$ is also a constant in space and time according to Eq. (38), i.e.:

$$\frac{\partial \rho^0 E^0}{\partial t} = \nabla \rho^0 E^0 = 0 \tag{40}$$

As shown in Ref. [5], the operator Δ_{il} obeys the following rules for the Roe average:

$$\Delta_{il}(\rho\phi) = \rho\Delta_{il}\phi + \phi\Delta_{il}\rho \tag{41}$$

Then the order 1 energy Eq. (36) can be deformed as

$$\tilde{\delta}\frac{\partial \rho_i^0 E_i^0}{\partial t} + \frac{1}{2}\sum_{l\in v(i)}(\rho_l^0 E_l^0 + p_l^0)\vec{\boldsymbol{u}}_l^0 \cdot \vec{\boldsymbol{n}}_{il} + |U_{il}^0|\Delta_{il}\rho^0 E^0 = 0$$

Upon introducing Eq. (40) and $p_i^0 = cte\ \forall \boldsymbol{i}$, it is easy to obtain:

$$u_{i+1,j}^0 - u_{i-1,j}^0 + v_{i,j+1}^0 - v_{i,j-1}^0 = 0 \tag{42}$$

Eq. (42) is the discretized version of Eq. (5). Therefore, the discrete solution by Low-Speed-Roe scheme supports the behaviour of velocity field described in Eq. (5).

The order 1 continuity Eq. (33) can be expressed as

$$\tilde{\delta}\frac{\partial \rho_i^0}{\partial t} + \frac{1}{2}(\rho_{i+1,j}^0 u_{i+1,j}^0 - \rho_{i-1,j}^0 u_{i-1,j}^0 + \rho_{i,j+1}^0 v_{i,j+1}^0 - \rho_{i,j-1}^0 v_{i,j-1}^0) + \frac{1}{2}\sum_{l\in v(i)}|U_{il}^0|\Delta_{il}\rho^0 = 0 \tag{43}$$

With the condition of Eq. (42), it is easy to know that a common solution of Eq. (43) should be

$$\rho^0 = Cte \tag{44}$$

However, it is difficult to prove that Eq. (44) is the unique solution of Eq. (43). In fact, as mentioned in Ref. [10], ρ^0 is not constant if entropy varies. Fortunately, without the trouble of checkerboard decoupling, it is easy to find numerical experiments supporting Eq. (44) provided that the initial entropy is constant and the initial density has non-trivial O(1) variations.

The behaviour of second order pressure (Eq. (6)) is studied in the end.

Adding Eqs. (34) and (35) as vectors and introducing Eq. (44), we can obtain:

$$\vec{\boldsymbol{i}}\frac{1}{2}\sum_{l\in v(i)}p_l^2(n_x)_{il}+\vec{\boldsymbol{j}}\frac{1}{2}\sum_{l\in v(i)}p_l^2(n_y)_{il}+\tilde{\delta}\frac{\rho_i^0\partial\vec{\boldsymbol{u}}_i^0}{\partial t}+\frac{1}{2}\rho_l^0\sum_{l\in v(i)}\vec{\boldsymbol{u}}_l^0\vec{\boldsymbol{u}}_l^0\cdot\vec{\boldsymbol{n}}_{il}+|U_{il}^0|\Delta_{il}\vec{\boldsymbol{u}}^0=0 \tag{45}$$

Divided by ρ_i^0 and then operated by the divergence operator, in Eq. (45) the time derivative terms of the velocity field will vanish according to Eq. (42). Consequently, with Eq. (44) taken into account, the following Eq. (46) can be obtained subject to the constant-entropy condition:

$$p_{i+2,j}^2+p_{i-2,j}^2+p_{i,j+2}^2+p_{i,j-2}^2-4p_{i,j}^2=f(\vec{x},\vec{\boldsymbol{u}}^0,\rho^0) \tag{46}$$

Eq. (46) is the discretized Poisson-type equation to describe the behaviour of p^2 just like Eq. (6) for the continuous case. It indicates that spatial pressure fluctuations in the discretized system not only scale with the square of the reference Mach number, but also actually satisfy the correct limit equations.

It is noticed that the subscripts of pressure in Eq. (46), such as $i-2$, $\boldsymbol{i}$ and $i+2$, imply odd–even decoupling, indicating that p^2 also suffers from the problem of checkerboard decoupling.

Now, let's see the order 1 energy equation of traditional preconditioned Roe scheme derived from Ref. [5] under the conditions $p_i^0=cte\ \forall\boldsymbol{i}$ and $p_i^1=cte\ \forall\boldsymbol{i}$:

$$\tilde{\delta}\frac{\partial\rho_i^0E_i^0}{\partial t}+\frac{1}{2}\sum_{l\in v(i)}(\rho_l^0E_l^0+p_l^0)\vec{\boldsymbol{u}}_l^0\cdot\vec{\boldsymbol{n}}_{il}+\frac{h_{il}^0}{\sqrt{Y_{il}^0}}U_{il}^0\rho_{il}^0\Delta_{il}U^0+\frac{2h_{il}^0}{\sqrt{Y_{il}^0}}\Delta_{il}p^2=0$$

According to Eqs. (34) and (35), we know that $\Delta_{il}p^2$ changes with time. Therefore, introducing Eq. (40) into the above equation, we can obtain:

$$u_{i+1,j}^0-u_{i-1,j}^0+v_{i,j+1}^0-v_{i,j-1}^0=-\frac{1}{\rho_l^0E_l^0+p_l^0}\sum_{l\in v(i)}\frac{h_{il}^0}{2\sqrt{Y_{il}^0}}U_{il}^0\rho_{il}^0\Delta_{il}U^0+\frac{h_{il}^0}{\sqrt{Y_{il}^0}}\Delta_{il}p^2\neq0 \tag{47}$$

Eq. (47) means that the velocity field does not satisfy the zero-Mach number divergence constraint in Eq. (5) for the system discretized by traditional preconditioned Roe scheme. Because the divergence constraint for velocity is one of the prerequisites for obtaining the Poisson-type equation of the second order pressure Eq. (6), the latter constraint is also not satisfied. According to these unexpected results, we can also conclude that Low-Speed-Roe scheme has better accuracy than traditional preconditioned Roe scheme.

The above discussions lead to the conclusion that Low-Speed-Roe scheme correctly reproduces the limiting behaviour of the continuous case, provided that the checkerboard modes in pressure and velocity can be controlled. In contrast, previously suggested preconditioned Roe schemes appear to violate the zero-velocity divergence constraint.

4.2. All-Speed-Roe scheme – an approximate analysis

This section gives a simple way to identify the behaviour of All-Speed-Roe scheme. As shown in Fig. 1, within the range $M<0.3$, $f(M)$ defined by Eq. (18) is roughly proportional to Mach number and can be approximated by

$$f(M)\approx\sqrt{5}M \tag{48}$$

Thus, the scheme Eq. (16) is deformed for low speeds:

$$\widetilde{\boldsymbol{F}}_{\mathrm{d},i+\frac{1}{2}}^{\text{A-Roe}}\approx-\frac{1}{2}\boldsymbol{R}_{i+\frac{1}{2}}\begin{bmatrix}|u| & & & \\ & |u| & & \\ & & (\sqrt{5}-1)|u| & \\ & & & (\sqrt{5}+1)|u|\end{bmatrix}_{i+\frac{1}{2}}\boldsymbol{R}_{i+\frac{1}{2}}^{-1}(\boldsymbol{Q}_{i+1}-\boldsymbol{Q}_i)\leqslant\left(\sqrt{5}+1\right)\widetilde{\boldsymbol{F}}_{\mathrm{d},i+\frac{1}{2}}^{\text{L-Roe}} \tag{49}$$

Eq. (49) means that the dissipation of All-Speed-Roe scheme will be no more than a few times those of Low-Speed-Roe scheme in the low Mach number limit. This essential feature of All-Speed-Roe scheme makes its behaviour similar to that of Low-Speed-Roe scheme.

Although it may be a deficiency that the dissipations of All-Speed-Roe scheme (Eqs. (16)–(18)) have larger margins than those of Low-Speed-Roe scheme, there has not been evidence of deteriorated resolutions so far. This problem can be further solved by choosing $f(M)$ another way. If we define $f(M) \to 0$ for low Mach number, All-Speed-Roe scheme approximately possesses the same numerical dissipation as Low-Speed-Roe scheme in the low Mach number limit.

4.3. All-Speed-Roe scheme – a general analysis

The approximate analysis mentioned above has revealed the essential feature of All-Speed-Roe scheme. In order to understand All-Speed-Roe scheme further, in this section we give a general analysis, which is valid for all of the concerned schemes. Firstly, we express pseudo-eigenvalues as

$$\lambda_{1,2}^{\text{A-Roe}} = U, \quad \lambda_3^{\text{A-Roe}} = f_1(M)c, \quad \text{and} \quad \lambda_4^{\text{A-Roe}} = f_2(M)c \tag{50}$$

Upon introducing Eq. (50) into Eq. (16), the dimensionless discrete governing equations for All-Speed-Roe scheme can be obtained as follows.

Continuity equation:

$$\tilde{\delta}\frac{\partial \rho_i}{\partial t} + \frac{1}{2}\sum_{l\in v(i)} \rho_l \vec{\boldsymbol{u}}_l \cdot \vec{\boldsymbol{n}}_{il} + |U_{il}|\left(\Delta_{il}\rho - \frac{1}{c_{il}^2}\Delta_{il}p\right) + \frac{1}{2M_*}\sum_{l\in v(i)} \bar{d}_1 \frac{1}{2c_{il}}\Delta_{il}p + \frac{1}{2}\sum_{l\in v(i)} \bar{d}_2 \rho_{il}\Delta_{il}U = 0 \tag{51}$$

Horizontal momentum equation:

$$\begin{aligned}&\frac{1}{2M_*^2}\sum_{l\in v(i)} p_l (n_x)_{il} + \tilde{\delta}\frac{\partial \rho_i u_i}{\partial t} + \frac{1}{2}\sum_{l\in v(i)} \rho_l u_l \vec{\boldsymbol{u}}_l \cdot \vec{\boldsymbol{n}}_{il} + |U_{il}|u_{il}\left(\Delta_{il}\rho - \frac{\Delta_{il}p}{c_{il}^2}\right) - (n_y)_{il}\rho_{il}|U_{il}|\Delta_{il}V \\ &+ \frac{1}{2M_*}\sum_{l\in v(i)} \bar{d}_1 \frac{u_{il}}{2c_{il}}\Delta_{il}p + \frac{1}{2M_*}\sum_{l\in v(i)} \bar{d}_1 (n_x)_{il}\rho_{il}c_{il}\Delta_{il}U + \frac{1}{2}\sum_{l\in v(i)} \bar{d}_2 \rho_{il}u_{il}\Delta_{il}U + \frac{1}{2M_*^2}\sum_{l\in v(i)} \bar{d}_2 (n_x)_{il}\Delta_{il}p = 0\end{aligned} \tag{52}$$

Vertical momentum equation:

$$\begin{aligned}&\frac{1}{2M_*^2}\sum_{l\in v(i)} p_l (n_y)_{il} + \tilde{\delta}\frac{\partial \rho_i v_i}{\partial t} + \frac{1}{2}\sum_{l\in v(i)} \rho_l v_l \vec{\boldsymbol{u}}_l \cdot \vec{\boldsymbol{n}}_{il} + |U_{il}|v_{il}\left(\Delta_{il}\rho - \frac{\Delta_{il}p}{c_{il}^2}\right) + (n_x)_{il}\rho_{il}|U_{il}|\Delta_{il}V \\ &+ \frac{1}{2M_*}\sum_{l\in v(i)} \bar{d}_1 \frac{v_{il}}{2c_{il}}\Delta_{il}p + \frac{1}{2M_*}\sum_{l\in v(i)} \bar{d}_1 (n_y)_{il}\rho_{il}c_{il}\Delta_{il}U + \frac{1}{2}\sum_{l\in v(i)} \bar{d}_2 \rho_{il}v_{il}\Delta_{il}U + \frac{1}{2M_*^2}\sum_{l\in v(i)} \bar{d}_2 (n_y)_{il}\Delta_{il}p = 0\end{aligned} \tag{53}$$

Energy equation:

$$\begin{aligned}&\tilde{\delta}\frac{\partial \rho_i E_i}{\partial t} + \frac{1}{2}\sum_{l\in v(i)} (\rho_l E_l + p_l)\vec{\boldsymbol{u}}_l \cdot \vec{\boldsymbol{n}}_{il} + \frac{M_*^2}{2}\sum_{l\in v(i)} |U_{il}|\frac{u_{il}^2 + v_{il}^2}{2}\left(\Delta_{il}\rho - \frac{\Delta_{il}p}{c_{il}^2}\right) + \rho_{il}|U_{il}|V_{il}\Delta_{il}V \\ &+ \frac{1}{2M_*}\sum_{l\in v(i)} \bar{d}_1 \frac{H_{il}}{2c_{il}}\Delta_{il}p + \frac{M_*}{2}\sum_{l\in v(i)} \bar{d}_1 U_{il}\rho_{il}c_{il}\Delta_{il}U + \frac{1}{2}\sum_{l\in v(i)} \bar{d}_2(\rho_{il}H_{il}\Delta_{il}U + U_{il}\Delta_{il}p) = 0\end{aligned} \tag{54}$$

Signals $\bar{d}_1 = |f_2(M)| + |f_1(M)|$, $\bar{d}_2 = |f_2(M)| - |f_1(M)|$ and $V = -un_y + vn_x$ are used in the above equations.

Upon choosing proper forms of $f_1(M)$ and $f_2(M)$ into Eqs. (51)–(54), the behaviour of specific scheme can be analyzed. Examples are given below.

(i) For "classical" Roe scheme, it holds that:

$$f_1 = \frac{U}{c} - 1 \quad \text{and} \quad f_2 = \frac{U}{c} + 1, \text{and thus}$$

$$\bar{d}_1 = 2 \quad \text{and} \quad \bar{d}_2 = 2\frac{U}{c} = 2M_*\frac{\widetilde{U}}{\tilde{c}}$$

Introducing these expressions into the governing equations we can obtain:

$$\sum_{l\in v(i)} \frac{\Delta_{il}p^0}{c^0_{il}} = 0 \tag{55}$$

$$p^0_{i-1,j} - p^0_{i+1,j} = 0 \tag{56}$$

$$p^0_{i,j-1} - p^0_{i,j+1} = 0 \tag{57}$$

$$\sum_{l\in v(i)} \frac{u^0_{il} + (n_x)_{il}U^0_{il}}{c^0_{il}}\Delta_{il}p^0 + (n_x)_{il}c^0_{il}\rho^0_{il}\Delta_{il}U^0 + \sum_{l\in v(i)} p^1_l(n_x)_{il} = 0 \tag{58}$$

$$\sum_{l\in v(i)} \frac{v^0_{il} + (n_y)_{il}U^0_{il}}{c^0_{il}}\Delta_{il}p^0 + (n_y)_{il}c^0_{il}\rho^0_{il}\Delta_{il}U^0 + \sum_{l\in v(i)} p^1_l(n_y)_{il} = 0 \tag{59}$$

Eqs. (55)–(57) imply that $p^0_i = cte\ \forall \boldsymbol{i}$ without possibility of velocity-pressure decoupling [5], and Eqs. (58) and (59) indicate that p^1_i is not a constant. Therefore, the discrete solution of Roe scheme supports pressure fluctuations of order M^*:

$$p(x,t) = P_0(t) + M_* p_1(x,t) \tag{60}$$

(ii) For Low-Speed-Roe scheme, it holds that $f_1 = f_2 = \frac{U}{c}$, and thus:

$$\bar{d}_1 = 2M_*\left|\frac{\widetilde{U}}{\tilde{c}}\right| \text{ and } \bar{d}_2 = 0$$

Accordingly, equations and conclusions in Section 4.1 can be obtained easily.

(iii) For All-Speed-Roe scheme Eqs. (16)–(18), it holds that:

$$f_1 = \frac{U}{c} - M\frac{\sqrt{4+(1-M^2)^2}}{1+M^2} \quad \text{and} \quad f_2 = \frac{U}{c} + M\frac{\sqrt{4+(1-M^2)^2}}{1+M^2}, \quad \text{and thus}$$

$$\bar{d}_1 = 2M_*\widetilde{M}\frac{\sqrt{4+(1-M_*^2\widetilde{M}^2)^2}}{1+M_*^2\widetilde{M}^2} \quad \text{and} \quad \bar{d}_2 = 2\frac{U}{c} = 2M_*\frac{\widetilde{U}}{\tilde{c}}$$

In order to research the pressure behaviour in the form of Eq. (4), the relevant terms with equal power of M^* in the governing equations are collected:

$$p^0_{i-1,j} - p^0_{i+1,j} = 0 \tag{61}$$

$$p^0_{i,j-1} - p^0_{i,j+1} = 0 \tag{62}$$

$$p^1_{i+1,j} - p^1_{i-1,j} + 2\sum_{l\in v(i)} \frac{(n_x)_{il}U^0_{il}}{c^0_{il}}\Delta_{il}p^0 = 0 \tag{63}$$

$$p^1_{i,j+1} - p^1_{i,j-1} + 2\sum_{l\in v(i)} \frac{(n_y)_{il}U^0_{il}}{c^0_{il}}\Delta_{il}p^0 = 0 \tag{64}$$

The forms of Eqs. (61) and (62) are exactly the same as those of Eqs. (29) and (30), also leading to the same conclusions that $p^0_i = cte\ \forall \boldsymbol{i}$ in physics but p^0 suffers from the four-field solution problem. If p^0 is a constant in space, Eqs. (63) and (64) of p^1 will have the same forms as Eqs. (61) and (62) for p^0. Then $p^1_i = cte\ \forall \boldsymbol{i}$ when excluding the possibility of the four-field solution. Therefore, the discrete solution of All-Speed-Roe scheme (16)–(18) supports pressure fluctuations of order M^2_* as shown in Eq. (37):

$$p(x,t) = P_0(t) + M_*^2 p_2(x,t)$$

With the conditions of $p_i^0 = cte\ \forall \boldsymbol{i}$ and $p_i^1 = cte\ \forall \boldsymbol{i}$ taken into account, the relevant terms of order 1 in energy Eq. (54) and continuity Eq. (51) and the vector sum of terms of order 1 in horizontal momentum Eq. (52) and vertical momentum Eq. (53) are collected as

$$\tilde{\delta}\frac{\partial \rho_i^0 E_i^0}{\partial t} + \frac{1}{2}\sum_{l\in v(i)} (\rho_l^0 E_l^0 + p_l^0)\vec{\boldsymbol{u}}_l^0 \cdot \vec{\boldsymbol{n}}_{il} = 0 \tag{65}$$

$$\tilde{\delta}\frac{\partial \rho_i^0}{\partial t} + \frac{1}{2}\sum_{l\in v(i)} \rho_l^0 \vec{\boldsymbol{u}}_l^0 \cdot \vec{\boldsymbol{n}}_{il} + |U_{il}^0|\Delta_{il}\rho^0 = 0 \tag{66}$$

$$\vec{\boldsymbol{i}}\frac{1}{2}\sum_{l\in v(i)} p_l^2 (n_x)_{il} + \vec{\boldsymbol{j}}\frac{1}{2}\sum_{l\in v(i)} p_l^2 (n_y)_{il} + \tilde{\delta}\frac{\rho_i^0 \partial \vec{\boldsymbol{u}}_i^0}{\partial t} + f(\vec{x}, \vec{\boldsymbol{u}}^0, \rho^0) = 0 \tag{67}$$

With the same logic used in Section 4.1, we can obtain the same results under the constant-entropy condition:

$$u_{i+1,j}^0 - u_{i-1,j}^0 + v_{i,j+1}^0 - v_{i,j-1}^0 = 0$$

$$\rho^0 = Cte$$

$$p_{i+2,j}^2 + p_{i-2,j}^2 + p_{i,j+2}^2 + p_{i,j-2}^2 - 4p_{i,j}^2 = f(\vec{\boldsymbol{x}}, \vec{\boldsymbol{u}}^0, \rho^0)$$

These results mean that discrete cases of the All-Speed-Roe scheme defined by Eqs. (16)–(18) has the same behaviour as continuous cases in the low Mach number and constant-entropy limit.

(iv) For a more general form of All-Speed-Roe scheme, the choice of factor $f(M)$ may be optimized.

In All-Speed-Roe scheme we simply multiply the sound speed term in eigenvalues of Roe scheme by a function $f(M)$ to remedy the accuracy problem. The form of $f(M)$ given in Eq. (18) is not the only one. Three empirical rules defining function $f(M)$ are given in Section 3.4. Further mathematic considerations will follow to provide more guidance for better choice in the low Mach number limit. We can express $f(M)$ as polynomials of M:

$$f_1(M) = \frac{U}{c} - \sum_{k=0}^{\infty} b_{1,k} M^k \quad \text{and} \quad f_2(M) = \frac{U}{c} + \sum_{k=0}^{\infty} b_{2,k} M^k$$

where $b_{1,k}$ and $b_{2,k}$ are arbitrary integer. For purpose of generality, we express:

$$\bar{d}_1 = \sum_{k=0}^{\infty} a_{1,k} M_*^k \widetilde{M}^k \quad \text{and} \quad \bar{d}_2 = \sum_{k=0}^{\infty} a_{2,k} M_*^k \widetilde{M}^k$$

where $a_{1,k}$ and $a_{2,k}$ are arbitrary integers.

Then, the relevant terms with equal powers of M^* are collected in order to research the behaviour of solutions in the form shown in Eq. (4):

$$p_{i+1,j}^0 - p_{i-1,j}^0 + \sum_{l\in v(i)} a_{2,0}(n_x)_{il}\Delta_{il}p^0 = 0 \tag{68}$$

$$p_{i,j+1}^0 - p_{i,j-1}^0 + \sum_{l\in v(i)} a_{2,0}(n_y)_{il}\Delta_{il}p^0 = 0 \tag{69}$$

$$\sum_{l\in v(i)} a_{1,0}\frac{\Delta_{il}p^0}{c_{il}^0} = 0 \tag{70}$$

$$p_{i+1,j}^1 - p_{i-1,j}^1 + \frac{1}{2}\sum_{l\in v(i)} a_{1,0}\frac{u_{il}^0}{c_{il}^0}\Delta_{il}p^0 + \sum_{l\in v(i)} a_{1,0}(n_x)_{il}\rho_{il}^0 c_{il}^0 \Delta_{il}U^0 + \sum_{l\in v(i)} a_{2,0}(n_x)_{il}\Delta_{il}p^1 + \sum_{l\in v(i)} a_{2,1}(n_x)_{il}\Delta_{il}p^0 = 0 \tag{71}$$

$$p_{i,j+1}^1 - p_{i,j-1}^1 + \frac{1}{2}\sum_{l\in v(i)} a_{1,0}\frac{v_{il}^0}{c_{il}^0}\Delta_{il}p^0 + \sum_{l\in v(i)} a_{1,0}(n_y)_{il}\rho_{il}^0 c_{il}^0 \Delta_{il}U^0 + \sum_{l\in v(i)} a_{2,0}(n_y)_{il}\Delta_{il}p^1 + \sum_{l\in v(i)} a_{2,1}(n_y)_{il}\Delta_{il}p^0 = 0 \tag{72}$$

Eqs. (68)–(70) are similar to those obtained from asymptotic analysis of preconditioned Roe scheme [5], and the same conclusion $p_i^0 = cte\ \forall \boldsymbol{i}$ can be obtained. Similarly, Eqs. (71) and (72) indicate that $p_i^1 = cte\ \forall \boldsymbol{i}$ if we are sure $a_{1,0} = 0$.In fact, $a_{1,0} = 0$ implies $a_{2,0} = 0$ because $a_{1,0} \geqslant a_{2,0}$, and the latter relation can be derived from the following expression:

$$\sum_{k=0}^{\infty} |a_{1,k}| M_*^k \widetilde{M}^k = |\bar{d}_1| = ||f_2(M)| + |f_1(M)|| \geqslant ||f_2(M)| - |f_1(M)|| = |\bar{d}_2| = \sum_{k=0}^{\infty} |a_{2,k}| M_*^k \widetilde{M}^k \tag{73}$$

Under the conditions of $p_i^0 = cte\ \forall \boldsymbol{i}$, $p_i^1 = cte\ \forall \boldsymbol{i}$, $a_{1,0} = 0$ and $a_{2,0} = 0$, the relevant terms with equal power of M^* have the same forms as shown in Eqs. (65)–(67). It means that the discrete solutions satisfy the limit Eqs. (5) and (6) if the entropy is assumed as constant.

Therefore, the sufficient and necessary condition for All-Speed-Roe scheme to possess necessary physical behaviour in the low Mach number regime is that the non-linear pseudo-eigenvalues satisfy the following rule:

$$|\lambda_3^{\text{A-Roe}}| + |\lambda_4^{\text{A-Roe}}| = |f_1(M)|c + |f_2(M)|c = c\sum_{k=1}^{\infty} a_k M^k \tag{74}$$

where a_k is an arbitrary integer.

For simplicity, we may set $f(M) = f_1(M) = f_2(M)$. It is easy to see that condition Eq. (74) will be satisfied by the following form of the factor:

$$f(M) = \sum_{k=1}^{\infty} a_k M^k \tag{75}$$

This more general form of the factor $f(M)$ can be used conveniently and be optimized for different purposes.

4.4. Further discussion on the checkerboard decoupling problem

The discussions above show that p^0, p^1 and p^2 all suffer from the problem of checkerboard decoupling for Low-Speed-Roe scheme and All-Speed-Roe scheme while "classical" Roe scheme avoid this trouble although it fails to satisfy the correct scaling of pressure fluctuations.

Paying attention again to Eqs. (68)–(70), we notice that checkerboard decoupling of p^0 would be suppressed if $a_{1,0} \neq 0$ and $a_{2,0} \neq 0$ because p^0 would satisfy homogeneous Poisson-type equations. An example is the expressions of traditional preconditioned Roe scheme given in Ref. [5]:

$$p_{i+1,j}^0 - p_{i-1,j}^0 + \sum_{l\in v(i)} \frac{(U^0 n_x + 2u^0)_{il}}{\sqrt{Y_{il}^0}} \Delta_{il} p^0 = 0 \tag{76}$$

$$p_{i,j+1}^0 - p_{i,j-1}^0 + \sum_{l\in v(i)} \frac{(U^0 n_y + 2v^0)_{il}}{\sqrt{Y_{il}^0}} \Delta_{il} p^0 = 0 \tag{77}$$

$$\sum_{l\in v(i)} \frac{\Delta_{il} p^0}{\sqrt{Y_{il}^0}} = 0 \tag{78}$$

which have much better ability to suppress checkerboard decoupling of p^0 than Eqs. (29) and (30), although not all checkerboard modes are suppressed as shown in the numerical experiments below.

However, as discussed in Section 4.3, $a_{1,0}$ and $a_{2,0}$ must be zero for Low-Speed-Roe scheme and All-Speed-Roe scheme. As a result, Eqs. (68)–(70) become Eqs. (29) and (30) and the discrete solutions have to suffer from serious checkerboard decoupling problem. This is why a pressure stabilization term as shown in Eq. (9) is inserted in the central term to provide a similar mechanism to suppress checkerboard mode. With Eq. (9) used as the central term, the corresponding equal power terms for p^0 are

$$p^0_{i+1,j} - p^0_{i-1,j} + \sum_{l\in v(i)} [a_{2,0}(n_x)_{il} + 2c_2\rho^0 u^0]\Delta_{il}p^0 = 0 \tag{79}$$

$$p^0_{i,j+1} - p^0_{i,j-1} + \sum_{l\in v(i)} [a_{2,0}(n_y)_{il} + 2c_2\rho^0 v^0]\Delta_{il}p^0 = 0 \tag{80}$$

$$\sum_{l\in v(i)} c_2\rho^0\Delta_{il}p^0 = 0 \tag{81}$$

Similar analysis is valid for p^1 and p^2.

Therefore, Low-Speed-Roe scheme and All-Speed-Roe scheme can avoid checkerboard mode as well as traditional preconditioned Roe scheme provided that the central term uses a form of momentum interpolation such as Eq. (9) or the combined form shown in Ref. [8].

Unfortunately, it is easy to know that the momentum interpolation like Eq. (9) leads to non-zero velocity divergences in the limit. The method of staggered grids may be a choice to avoid this embarrassment. However, in order to lessen the programming effort, an improved momentum interpolation method for this limitation still deserves to be researched further.

5. Numerical experiments

In order to further examine the ability of All-Speed-Roe scheme for low Mach number flows, the inviscid flow past a high-loaded turbine blade (T106) row is simulated. MUSCL reconstruction is applied for second order accuracy. The mesh is adopted with 40*98 grid points in azimuthal and streamwise directions.

Fig. 3 shows the contours of pressure at a very low inlet Mach number (0.001), which are calculated with the central term in the form of Eq. (8). Obviously, the twisted pressure field can be seen in Fig. 3(a), indicating that original Roe scheme creates numerical dissipations in the low Mach number simulation, which is too severe to give a physical solution. The problem of checkerboard decoupling, however, does not appear here. A reasonable solution is calculated by traditional preconditioned Roe scheme as shown in Fig. 3(b). However some small wiggle patterns in the pressure contours can be noticed, indicating that traditional preconditioned Roe scheme cannot suppress the checkerboard modes totally. In fact, this deficiency is attributed to the momentum interpolation itself. Fig. 3(c) provides a typical picture of checkerboard decoupling obtained by All-Speed-Roe scheme with the construction of Eqs. (8), (16), (17) and (18). It is obvious that traditional preconditioned Roe scheme is much better than All-Speed-Roe scheme in avoiding the checkerboard decoupling.

Applying momentum interpolation with $c_2 = 0.05$ (Eq. (9)), All-Speed-Roe scheme gets great improvement in the problem of checkerboard decoupling, as shown in Fig. 4(b), whereas the result in Fig. 4(a) by traditional preconditioned Roe scheme is scarcely improved because the improving mechanism of Eq. (9) is similar to that of preconditioned Roe scheme. Except for the effects of checkerboard decoupling, the contours by precondi-

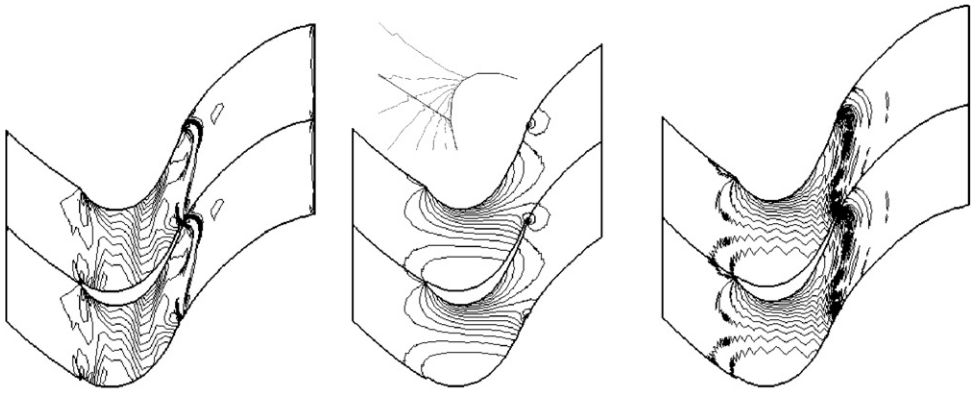

Fig. 3. Pressure contours at inlet Mach number 0.001, simple form of the central term is used.

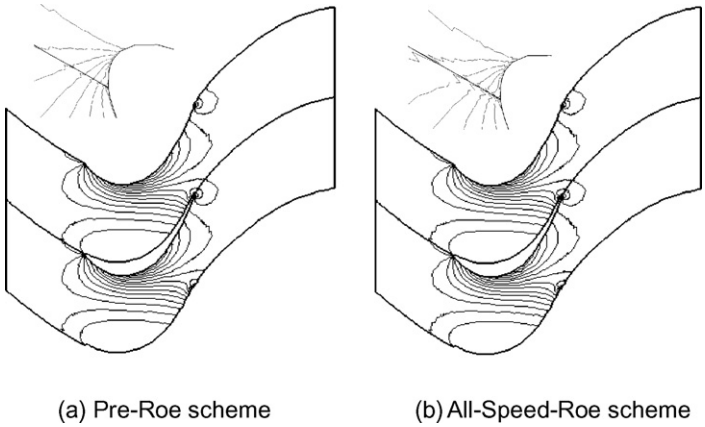

Fig. 4. Pressure contours at inlet Mach number 0.001, a pressure stabilization term is used in the central term.

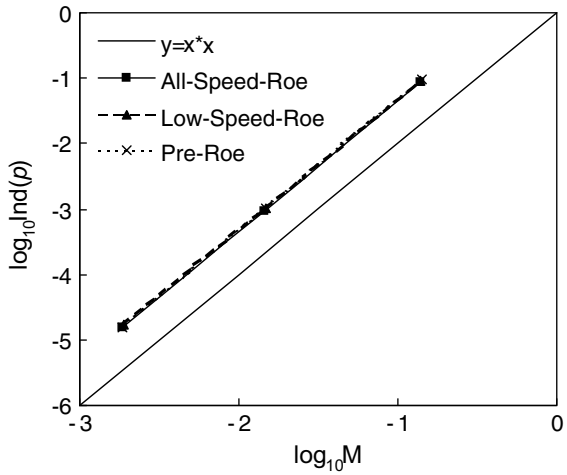

Fig. 5. Pressure fluctuations vs inflow Mach number.

tioned Roe and All-Speed-Roe schemes are undistinguishable from each other. It means that results by modified Roe schemes converge to a unique reasonable solution.

Fig. 5 displays the pressure fluctuations $\mathrm{Ind}(p) = (P_{\max} - P_{\min})/P_{\max}$ vs the inlet Mach number when Eq. (9) is used as the central term. Results by Low-Speed-Roe and All-Speed-Roe schemes perfectly agree with the theoretical asymptotic predictions: the pressure fluctuations scale exactly with M_*^2 both in the continuous case and in the preconditioned and relevant improved discrete cases.

6. Conclusions

In this paper, a numerical scheme for all-speed flows is developed, the idea of which is to simply multiply the acoustic term c in eigenvalues of the present shock-capturing schemes by a factor $f(M)$ to remedy their accuracy problems. An asymptotic analysis leads to the following conclusions:

(1) The supposed All-Speed-Roe scheme has the same behaviour in low Mach number limit as the original governing equations in the continuous case – the following important characteristics are held for its discrete equations:

(a) Pressure fluctuations scale with the square of the Mach number. This conclusion is also confirmed by numerical experiments.
(b) The zero order velocity is subject to a divergence constraint.
(c) The second order pressure fluctuations satisfy a Poisson-type equation under the constant-entropy condition.

For a discrete case, characteristics (b) and (c) are researched for the first time, although characteristic (a) has been tackled by many predecessors [5,6,11]. An unexpected conclusion is also obtained that conditions (b) and (c) are not satisfied by the discretized equations of traditional preconditioned Roe scheme.

(2) All-Speed-Roe scheme, unlike traditional preconditioned Roe scheme, does not have an inherent mechanism to suppress checkerboard decoupling. Instead, adding pressure stabilization terms to the interface fluid velocity as done in Eq. (9) can also provide a similar mechanism.
(3) The choice of the function $f(M)$ is not unique in All-Speed-Roe scheme, which will have the correct physical behaviour as long as $f(M)$ takes the form $f(M) = \min\left(\sum_{k=1}^{\infty} a_k M^k, 1\right)$. Its specific structures optimized for accuracy and/or stability deserve further researches.

In summary, the proposed All-Speed-Roe scheme has a sound foundation for further development and engineering applications.

Acknowledgments

This work is supported by Project 50776051 of National Natural Science Foundation of China, Project 2007CB210105 of 973 Program, and Project 20060400424 of China Postdoctoral Science Foundation.

The authors are heartily grateful to the reviewers for their helpful suggestions, especially for the discussions about Eqs. (5) and (6), addition of which is suggested by a reviewer.

References

[1] J.M. Weiss, W.A. Smith, Preconditioning applied to variable and constant density flows, AIAA Journal 33 (1995) 2050–2057.
[2] J.R. Edwards, M.S. Liou, Low-diffusion flux-splitting methods for flows at all speeds, AIAA Journal 36 (1998) 1610–1617.
[3] E. Turkel, Preconditioning techniques in computational fluid dynamics, Annual Reviews of Fluid Mechanics 31 (1999) 385–416.
[4] I. Mary, P. Sagaut, M. Deville, An algorithm for unsteady viscous flows at all speeds, International Journal for Numerical Methods in Fluids 34 (2000) 371–401.
[5] H. Guillard, C. Viozat, On the behaviour of upwind schemes in the low mach number limit, Computers and Fluids 28 (1999) 63–86.
[6] H. Guillard, A. Murrone, On the behaviour of upwind schemes in the low mach number limit: II. Godunov type schemes, Computers and Fluids 33 (2004) 655–675.
[7] P. Birken, A. Meister, Stability of preconditioned finite volume schemes at low mach numbers, Numerical Mathematics 45 (2005) 463–480.
[8] X.S. Li, C.W. Gu, J.Z. Xu, Research of preconditioned roe scheme for all speed flows in turbomachinery, in: ISABE Conference of AIAA, 2007-1113.
[9] S. Klainerman, A. Majda, Compressible and incompressible fluids, Communications on Pure Applied Mathematics 35 (1982) 629–651.
[10] R. Klein, Semi-implicit extension of a Godunov-type scheme based on low mach number asymptotics I: One-dimensional flow, Journal of Computational Physics 121 (1995) 213–237.
[11] A. Meister, Asymptotic based preconditioning technique for low mach number flows, Zeitschrift fur Angewandte Mathematik und Mechanik 83 (1) (2003) 3–25.
[12] C.M. Rhie, W.L. Chow, Numerical study of the turbulent flow past an airfoil with trailing edge separation, AIAA Journal 21 (1983) 1525–1532.
[13] I. Mary, P. Sagaut, Large eddy simulation of flow around an airfoil near stall, AIAA Journal 40 (2002) 1139–1145.
[14] D.L. Darmofal, P.J. Schmid, The importance of eigenvectors for local preconditioners of the euler equations, Journal of Computational Physics 127 (1996) 346–362.
[15] X.S. Li, Large Eddy Simulation Based on the Computational Method of Compressible Flows and its Application to Engineering, Ph.D. Dissertation, Institute of Engineering Thermophysics, Chinese Academy of Sciences, Beijing, March 2006.
[16] X.S. Li, J.Z. Xu, C.W. Gu, Preconditioning method and engineering application of large eddy simulation. Science in China Series G: Physics, Mechanics & Astronomy (2008), doi:10.1007/s11433-008-0054-1.
[17] S.H. Lee, Cancellation problem of preconditioning method at low mach numbers, Journal of Computational Physics 225 (2007) 1199–1210.